Dual-frequency terahertz emission from splitting filaments induced by lens tilting in air

Zhelin Zhang[1], Yanping Chen[1,a)], Liu Yang[1], Xiaohui Yuan[1], Feng Liu[1], Min Chen[1], Jianqiu Xu[1], Zhengming Sheng[1,2], and Jie Zhang[1]

[1]*Key Laboratory for Laser Plasmas (Ministry of Education), Department of Physics and Astronomy, Shanghai Jiao Tong University, Shanghai 200240, China*
[2]*Department of Physics, SUPA, University of Strathclyde, Glasgow G4 0NG, UK*

Abstract

Dual-frequency terahertz radiation from air-plasma filaments produced with two-color lasers in air has been demonstrated experimentally. When a focusing lens is tilted for a few degrees, it is shown that the laser filament evolves from a single one to two sub-filaments. Two independent terahertz sources emitted from the sub-filaments with different frequencies and polarizations are identified, where the frequency of terahertz waves from the trailing sub-filament is higher than that from the leading sub-filament.

[a)]Author to whom correspondence should be addressed; electronic mail: yanping.chen@sjtu.edu.cn

Terahertz (THz) radiation from femtosecond laser induced air-plasma filaments has attracted significant interests during the past few decades due to its widely spanned potential applications, such as material spectroscopy, biological imaging and characterization, security protection, etc. [1-3] As a special medium for terahertz generation, the air-plasma filaments can be generated close to a remote target by manipulating their locations, minimizing the strong absorption by water vapor in the atmosphere between the THz sources and the detecting targets. Besides, it refrains from the shortcoming of damage threshold in solid medium. Since the first demonstration of terahertz radiation from such filaments [4], lots of efforts have been made towards understanding and optimization of this terahertz emission by controlling experimental parameters that affect the formation of the filaments. Introductions of a second-harmonic crystal and a dc bias voltage are effective ways to improve the intensity of terahertz emission from filaments [5-11]. Terahertz radiation can also be enhanced by 1 order of magnitude when two filaments were concatenated to a single longer filament [12]. The divergence of terahertz radiation can be optimized by increasing the length of the filaments [13, 14]. Efficient frequency tuning has been demonstrated by modification of the plasma density inside the filaments [15]. Besides, shortening of terahertz pulses was obtained from a uniform plasma string by tailoring its spatial distribution [16]. This result indicates that the property of the terahertz emission from filaments also depends on the uniformity of the plasma distribution along a filament. Therefore, it is also interesting to learn how the terahertz radiation from a filament will evolve when its spatial uniformity of the plasma is deteriorated, one of which is breaking-up of a plasma string [17].

In this Letter, we demonstrate dual-frequency terahertz radiation emitted from filaments whose spatial distributions are reorganized by tilting a converging lens. These two independent terahertz sources, featuring with different frequencies and polarizations, are generated when a filament splits into two sub-filaments due to astigmatism effect.

The experimental setup is illustrated in Fig. 1. A 1 kHz, 40 fs Ti-sapphire laser beam was focused by a plano-convex lens with 30 cm focal length, creating filaments in air. The pump energy was 3.5 mJ, horizontally polarized. The plano-convex lens is fixed on a rotary mount so that the angle of incidence can be changed by tilting the lens along its vertical axis. Thus, the spatial distribution of the filament can be modified by rotating the lens, which was recorded by a CCD camera. To improve THz radiation from the filament, a 150-μm-thick β-barium borate (BBO) crystal cut for type I second-harmonic generation was added into the beam for frequency doubling to 400 nm, resulting in a two-color filament. The orientation of the BBO crystal was set where the terahertz generation from the two-color filament was optimized. The terahertz emission from the two-color filament was collected and probed by an electro-optic sampling (EOS) device, which was detailed in previous literature [18]. The thickness of the ZnTe crystal is 1.5 mm. The polarization of the terahertz pulses was analyzed by a wire grid polarizer.

Reorganization of the plasma distribution along a filament is carried out by introducing astigmatism [19] through lens tilting. Figure 2 illustrates the evolution of the filament spatial profile as a function of the tilting angle of the plano-convex lens. The laser beam propagates from left to right and travels parallel to the principal axis of the converging lens when the tilting angle is 0º. When the lens is tilted, laser beams propagating in two perpendicular planes have different foci. The larger the tilting angle is, the more astigmatism it introduces, and the further the foci depart from each other. As a consequence, stretch of the filament is observed while slightly increasing the tilting angle by rotating the lens with respect to its vertical axis, as shown in Figs. 2(b) and 2(c). When the tilting angle reaches 7º, the filament splits into two parts, a leading sub-filament (closer to the converging lens) and a trailing one, as shown in Fig. 2(d).

The THz emission from the two-color filaments is detected by the EOS device and the Fourier transform terahertz spectra are illustrated in Fig 3. The spectrum peaks at 0.9 THz at lens tilting angle of 0° (normal incidence). This spectral peak stays almost constant when increasing the tilting angle to 3° and 5°. When the tilting angle increases to 7°, this peak shifts to 1 THz and a new spectral peak appears at 0.4 THz. This observation suggests that the splitting of the filament modifies the spectral characteristic of terahertz emission from the two-color filament. To further clarify the relationship between terahertz spectral evolution and filament splitting, a metal iris with a 1.3-mm-aperture is applied in the middle of the two sub-filaments, as shown in Fig. 4. This aperture is large enough to survive the two-color filament. Meanwhile, most of the terahertz radiation generated before the metal iris is blocked as THz radiation from air filament is in a cone-shape [13, 14]. The spectral properties of the terahertz emission from the two-color air-filament with the metal iris scanned from the beginning to the end of the leading sub-filament are summarized in Fig. 4. The solid line is terahertz spectrum obtained when the metal iris locating at the beginning of the leading sub-filament (0 mm), which can be considered as a sum of terahertz emission from the leading and the trailing sub-filaments. It features with two pronounced peaks at 0.4 THz and 1 THz, respectively. The peak at 0.4 THz starts to decrease when the metal iris is scanned from the beginning of the leading sub-filament, i.e., terahertz radiation from the leading sub-filament is partially blocked, as dotted line and dash-dot line shown in Fig. 4. Its amplitude decreases by 4/5 when the metal iris locates 8 mm away from the beginning of the leading sub-filament while the decrease in the spectral peak at 1 THz is negligible, as shown by the dashed line in Fig. 4. As a consequence, one may conclude that the spectral peak around 0.4 THz represents terahertz emission from the leading sub-filament as its amplitude changes while the metal iris scans along the leading sub-filament. And the spectral peak at 1 THz relates to terahertz radiation from the trailing sub-filament. In a plasma current model for two-color laser fields, electron drifting current from field ionization is accounted for terahertz generation [20-22]. The frequency of terahertz radiation from an air-filament corresponds to the local plasma frequency, i.e., terahertz frequency is in close relationship with plasma density through the equation $\omega_{pe} = \sqrt{e^2 n_e / m_e \varepsilon_0}$ where ω_{pe} represents the plasma frequency, n_e is the plasma density, ε_0 is the vacuum dielectric coefficient, and e and m_e are the charge and mass of the electron, respectively. This means that the plasma densities in two sub-filaments are quite different. Referring to the above equation, the calculated plasma density for the leading sub-filament is around 2.0 x 10^{15} cm^{-3} [15]. For the trailing sub-filament, it possesses a higher plasma density than the leading one, around 1.2 x 10^{16} cm^{-3}.

The polarization properties of the THz emission from two-color filaments obtained with lens tilting angle of 0°, 3°, 5° and 7° are summarized in Fig. 5. Each solid square/triangle in polarization diagrams represents peak-to-peak amplitude of the terahertz electric field measured at one specified polarization direction defined by the orientation of the terahertz polarizer. The EOS detection itself is also sensitive to terahertz polarization as a linear polarizer. Therefore, the terahertz emission will obey a squared Malus Law: $I \propto \cos^4(\phi)$, i.e., $\mathrm{E} \propto \cos^2(\phi)$, where I and E represent the intensity and the amplitude of the terahertz signal, if it is linearly polarized. It is obvious, however, the measured terahertz signal is not purely linearly polarized as the polarization curve does not reach zero. We fit the terahertz polarization curves by using the following equation

$$E = \cos^2(\phi + \phi_0) + \alpha^2 \sin^2(\phi + \phi_0) \tag{1}$$

in polar coordinates, where E represents the amplitude of the terahertz signal, α is the elliptical ratio parameter ($\alpha = E_{THz,MinorAxis} / E_{THz,MajorAxis}$), and ϕ_0 is the angle between the maximum transmission of the terahertz analyzer and the pump polarization. Thus, the origin (ϕ=0°) is set for transmission of horizontally polarized terahertz pulses. Before the filament splitting into two sub-filaments, the polarization curve can be well fitted by Eq. (1) with α = 0.2 and ϕ_0=21°, 25°, 26° for lens tilting angle of 0°, 3° and 5°, as shown in Figs. 5(a)-5(c). This observation collaborates with the result in previous literature that THz radiation from a two-color filament is elliptically polarized [23]. When filament splitting occurs at lens tilting angle of 7°, another minor polarization component occurs, which happens to nearly perpendicular to the major one, as solid squares in Fig. 5(d). This minor polarization component can be well suppressed when most of the THz radiation from the leading sub-filament is blocked by locating the metal iris in the middle of these two sub-filaments, as solid triangles in Fig. 5(d). The major polarization component, representing THz radiation from the trailing sub-filament, again fits well with elliptical polarization. Therefore, the emergence of the second polarization component can be interpreted as the consequence of filament splitting, i.e., the THz radiations from the leading and the trailing sub-filaments have independent polarization properties. This observation could be due to different polarization statuses of the 400 nm beam while it propagates inside the leading and the trailing sub-filaments as the polarization of the terahertz radiation from a two-color filament is quite sensitive to the polarization of the 400 nm beam [24]. In our experiment, the linearly polarized 400 nm beam sees the birefringence of the air caused by the femtosecond laser filament [25], its polarization turns to elliptically polarized after it passes through the leading sub-filament. Consequently, the polarization difference of the 400 nm beam entering the leading and the trailing sub-filaments leads to the polarization difference of the terahertz radiation from these two sub-filaments.

In conclusion, we demonstrated that dual-frequency terahertz radiation from a two-color filament by splitting the filament into two sub-filaments through lens tilting induced astigmatism.

These two spectral components are independent terahertz sources, showing different frequencies and polarizations. The frequency of the terahertz waves emitted from the leading sub-filament is lower than that from the trailing one. This work enriches the knowledge of terahertz radiations produced by a two-color filament in air, gives one a vivid picture about the terahertz pulses radiating from two successive filaments, and suggests alternative control of terahertz emission simply by tilting a converging lens. This also provides a possibility of offering a dual-frequency terahertz source which might be interesting for terahertz applications such as THz antennas and THz communications.

This work was supported by the National Basic Research Program of China (No. 2014CB339800) and the National Natural Science Foundation of China (Nos. 11104259, 11474202 and 11121504).

References:

1. Q. Wu and X.-C. Zhang, Appl. Phys. Lett. **67**, 3523 (1995).
2. J. H. Booske, Phys. Plasmas **15**, 055502 (2008).
3. P. H. Siegel, IEEE Trans. Microwave Theory Tech. **50**, 910 (2002).
4. H. Hamster, A. Sullivan, S. Gordon, W. White, and R. W. Falcone, Phys. Rev. Lett. **71**, 2725 (1993).
5. D.J. Cook, R.M. Hochstrasser, Opt. Lett. **25**, 1210 (2000).
6. X. Xie, J. Dai, X.-C. Zhang, Phys. Rev. Lett. **96**, 075005 (2006).
7. K.Y. Kim, A.J. Taylor, J.H. Glownia, G. Rodriguez, Nature Photonics **2**, 605 (2008).
8. T. Loffler, F. Jacob, and H. G. Roskos, Appl. Phys. Lett. **77**, 453 (2000).
9. A. Houard, Y. Liu, B. Prade, V. T. Tikhonchuk, and A. Mysyrowicz, Phys. Rev. Lett. **100**, 255006 (2008).
10. Y. Chen, T. Wang, C. Marceau, F. Théberge, M. Châteauneuf, J. Dubois, O. Kosareva, and S. L. Chin, Appl. Phys. Lett. **95**, 101101 (2009).
11. T. Wang, C. Marceau, Y. Chen, S. Yuan, F. Theberge, M. Chateauneuf, J. Dubois and S. L. Chin, Appl. Phys. Lett. **96**, 211113 (2010).
12. J.-M. Manceau, M. Massaouti, and S. Tzortzakis, Opt. Lett. **35**, 2424 (2010).
13. H. Zhong, N. Karpowicz, and X. C. Zhang, Appl. Phys. Lett. **88**, 261103 (2006).
14. C. D'Amico, A. Houard, M. Franco, B. Prade, A. Mysyrowicz, A. Couairon, and V. T. Tikhonchuk, Phys. Rev. Lett. **98**, 235002 (2007).
15. Y. Chen, T. Wang, C. Marceau, F. Théberge, M. Châteauneuf, J. Dubois, O. Kosareva, and S. L. Chin, Appl. Phys. Lett. **95**, 101101 (2009).

16. J.-M. Manceau, A. Averchi, F. Bonaretti, D. Faccio, P. Di Trapani, A. Couairon, and S. Tzortzakis, Opt. Lett. **34**, 2165 (2009).

17. Y. Kamali, Q. Sun, J.-F. Daigle, A. Azarm, J. Bernhardt, and S.L. Chin, Opt. Commun. **282**, 950 (2009).

18. Y. Chen, C. Marceau, W. Liu, Z.-D. Sun, Y. Zhang, F. Théberge, M. Châteauneuf, J. Dubois and S.L. Chin, Appl. Phys. Lett. **93**, 231116 (2008).

19. H. H. Hopkins, Wave Theory of Aberrations, Clarendon Press, Oxford, 1950, chap. 5, “Astigmatism”.

20. K. Y. Kim, J. H. Glownia, A. J. Taylor, and G. Rodriguez, Opt. Express **15**, 4577 (2007).

21. M. Chen, A. Pukhov, X.-Y. Peng, and O. Willi, Phys. Rev. E **78**, 046406 (2008).

22. W.M. Wang, Y.T. Li, Z.M. Sheng, X. Lu, and J. Zhang, Phys. Rev. E **87**, 033108 (2013).

23. Y. Chen, C. Marceau, S. Génier, F. Théberge, M. Châteauneuf, J. Dubois, S. L. Chin, Opt. Commun. **282**, 4283 (2009).

24. A. Houard, Y. Liu, B. Prade, A. Mysyrowicz, Opt. Lett. **33**, 1195 (2008).

25. C. Marceau, Y. Chen, F. Théberge, M. Châteauneuf, J. Dubois, and S. L. Chin, Opt. Lett. **34**, 1417 (2009).

Figure Captions:

Fig. 1. (Color online) Schematic illustration of the experimental setup.

Fig. 2. (Color online) Some typical pictures taken by CCD camera at the lens tilting angle of (a) 0º, (b) 3º, (c) 5º, (d) 7º, respectively. The arrow indicates the propagation direction of the laser pulse. N is number of laser shots for each picture.

Fig. 3. (Color online) Terahertz spectral amplitudes obtained by Fourier transforms with the lens tilting angle of 0º, 3º, 5º, 7º, respectively.

Fig. 4. (Color online) Terahertz spectral amplitudes at the lens tilting angle of 7º with iris locating at 0 mm (solid line), 4 mm (dotted line), 6 mm (dash-dot line) and 8 mm (dashed line) away from the beginning of the leading sub-filament.

Fig. 5. (Color online) Polarizations of the terahertz pulses measured at the lens tilting angle of (a) 0º, (b) 3º, (c) 5º and (d) 7º, respectively. Solid lines are fitting curves.

Figure 1:

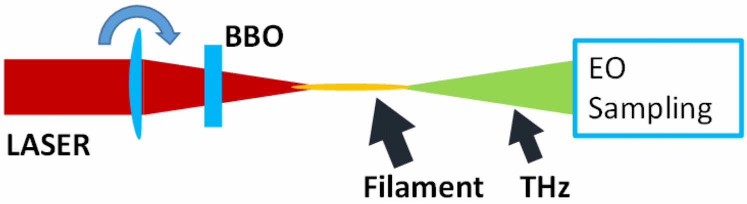

Figure 2:

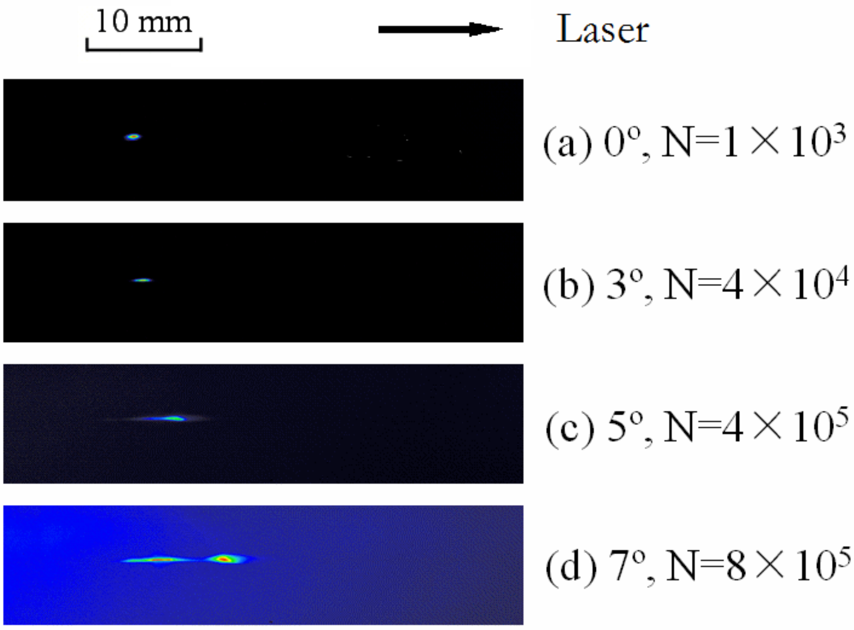

Figure 3:

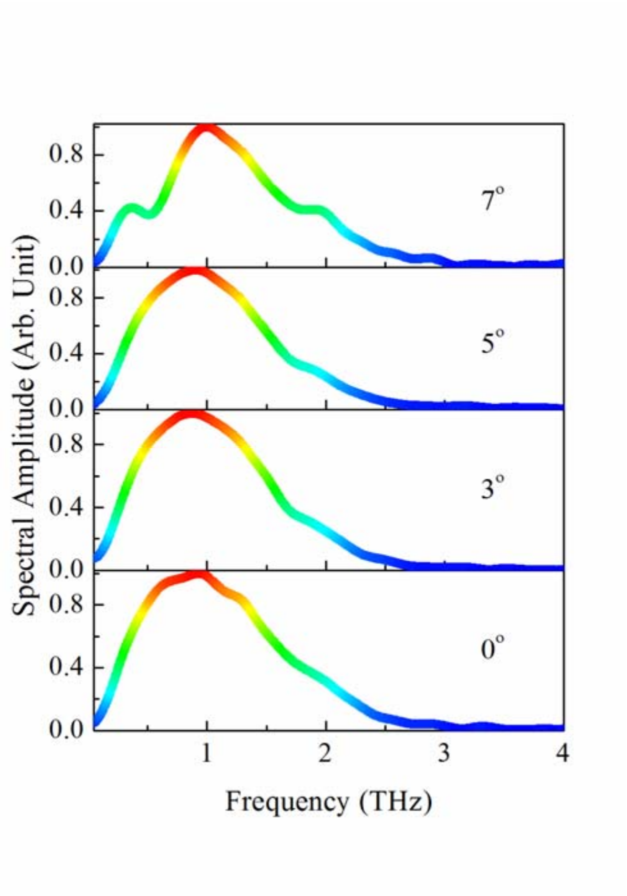

Spectral Amplitude (Arb. Unit)
0.0
0.4
0.8
7°
5°
3°
0°
1
2
3
4
Frequency (THz)

Figure 4:

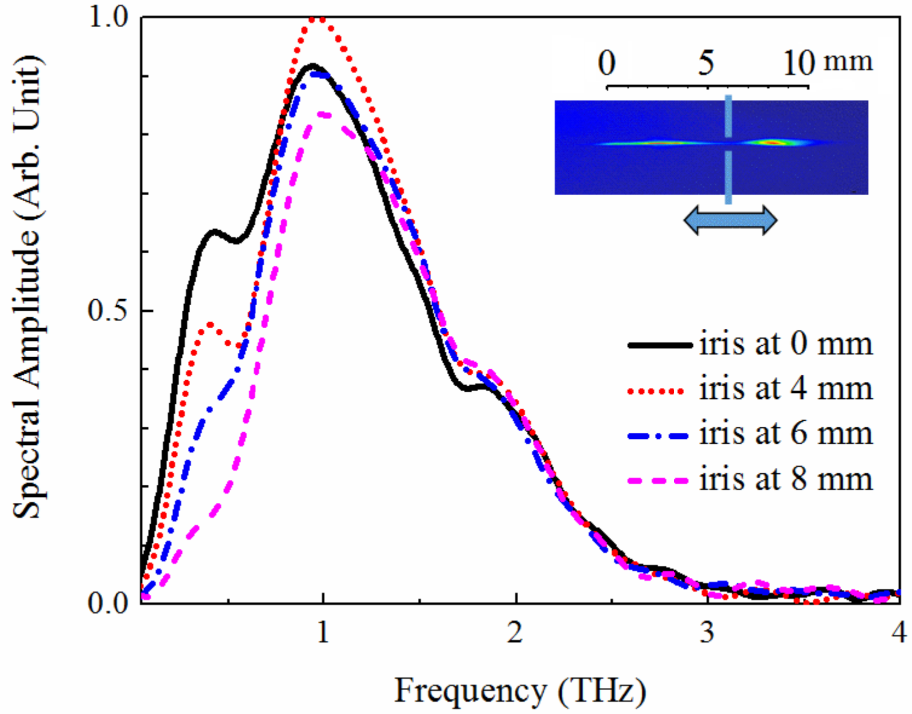
1.0
0.5
0.0
1
2
3
4
Spectral Amplitude (Arb. Unit)
Frequency (THz)
0
5
10 mm
iris at 0 mm
iris at 4 mm
iris at 6 mm
iris at 8 mm

Figure 5:

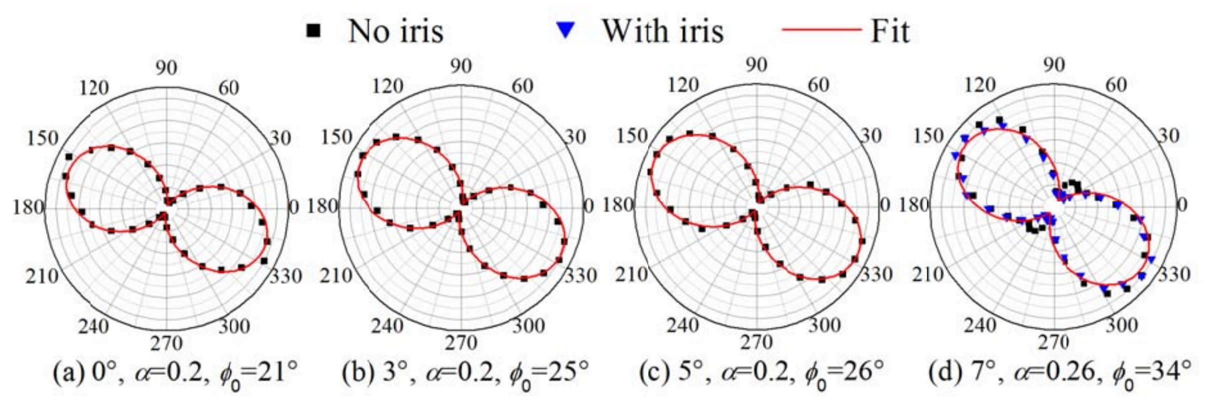

No iris
With iris
Fit
90
120
60
150
30
180
0
210
330
240
300
270
(a) 0°, α=0.2, φ0=21°
(b) 3°, α=0.2, φ0=25°
(c) 5°, α=0.2, φ0=26°
(d) 7°, α=0.26, φ0=34°